

Synthesis and Spectroscopic Characterization of Photo-affinity Peptide Ligands to Study Rhodopsin–G Protein Interaction[†]

Yihui Chen^{†1}, Rolf Herrmann^{‡2}, Nathan Fishkin^{¶1}, Peter Henklein³, Koji Nakanishi^{*1} and Oliver P. Ernst^{*2}

¹Department of Chemistry, Columbia University, New York, NY

²Institut für Medizinische Physik und Biophysik, Charité-Universitätsmedizin Berlin, Berlin, Germany

³Institut für Biochemie, Charité-Universitätsmedizin Berlin, Berlin, Germany

Received 31 October 2007, accepted 11 December 2007, DOI: 10.1111/j.1751-1097.2008.00304.x

ABSTRACT

G protein-coupled receptors (GPCRs) are involved in the control of virtually all aspects of our behavior and physiology. Activated receptors catalyze nucleotide exchange in heterotrimeric G proteins (composed of α -GDP, β and γ subunits) on the inner surface of the cell membrane. The GPCR rhodopsin and the G protein transducin (G_t) are key proteins in the early steps of the visual cascade. The main receptor interaction sites on G_t are the C-terminal tail of the $G_t\alpha$ -subunit and the farnesylated C-terminal tail of the $G_t\gamma$ -subunit. Synthetic peptides derived from these C-termini specifically bind and stabilize the active rhodopsin conformation (R^*). Here we report the synthesis of R^* -interacting peptides containing photo-reactive groups with a specific isotope pattern, which can facilitate detection of cross-linked products by mass spectrometry. In a preliminary set of experiments, we characterized such peptides derived from the farnesylated $G_t\gamma$ C-terminus ($G_t\gamma(60-71)$ far) in terms of their capability to bind R^* . Here, we describe novel peptides with photo-affinity labels that bind R^* with affinities similar to that of the native $G_t\gamma(60-71)$ far peptide. Such peptides will enable an improved experimental strategy to probe rhodopsin– G_t interaction and to map so far unknown interaction sites between both proteins.

INTRODUCTION

G protein-coupled receptors (GPCRs) are one of the most versatile families of proteins and respond as cell-surface receptors to endogenous signals in the form of chemically diverse small molecules. Ligand binding to the receptor stabilizes the active receptor conformation (R^*), which catalyzes GDP \rightarrow GTP exchange in heterotrimeric G proteins (composed of α -GDP, β and γ subunits) on the inner surface of the cell membrane (1,2). The GPCR superfamily plays an important role in many physiologic and pathophysiologic

processes. Accordingly, numerous drugs from the past and present target membrane-bound GPCRs (3).

In visual signal transduction in rod photoreceptors, the GPCR rhodopsin with its covalently bound chromophore 11-*cis*-retinal acts as the photon detector. Light absorption causes *cis* \rightarrow *trans* isomerization and thereupon *in situ* formation of an activating ligand in rhodopsin's chromophore binding site. Rhodopsin and its cognate G protein transducin (G_t) represent the only GPCR/G protein system for which crystal structures are available (4–7). Different models of receptor/G protein interaction were proposed on the basis of a variety of experimental and theoretical approaches (8–22). However, the detailed molecular mechanism of signal transfer between these two proteins leading to nucleotide exchange is not clear. Several putative interaction sites on G_t have been reported but only two of them (depicted in orange in Fig. 1), *i.e.* the C-terminal tail of $G_t\alpha$ ($G_t\alpha(340-350)$) and the farnesylated C-terminal tail of $G_t\gamma$ ($G_t\gamma(60-71)$ far), have been shown to specifically bind and stabilize the active conformation of rhodopsin (R^*), called metarhodopsin II (MII) (18,23). Synthetic peptides corresponding to $G_t\alpha(340-350)$ (IKENLKDCGLF) and $G_t\gamma(60-71)$ far (DKNPFKELKGGC-farnesyl) mimic the G_t holoprotein and bind in a similar manner to MII. NMR studies showed that both peptides adopt helical conformations upon receptor binding (24,25). In Fig. 1, additional potential binding sites on G_t are facing toward the cytoplasmic interaction surface of rhodopsin (for a review, see Hamm [11]). G_t 's C-terminal $\alpha 5$ helix with the $G_t\alpha(340-350)$ tail was identified as the key determinant for G_t -binding to R^* and GDP release from $G_t\alpha$ (12,18,21,26,27). It was proposed that $G_t\gamma(60-71)$ far constitutes together with the myristoylated $G_t\alpha$ N-terminus (myristate shown in gray in Fig. 1) an amphiphilic microdomain. This microdomain forms a docking complex with R^* upon the initial encounter (20). Upon docking, $G_t\alpha(340-350)$ becomes available for key interaction with R^* , resulting in the termination of the $R^*/G_t\gamma(60-71)$ interaction (19,20).

Although modeling approaches led to various 3D models of the R^*G_t complex with different R^*/G_t stoichiometries including rhodopsin mono-, di- or tetramers (28–31), the relative orientation of G_t and R^* is not known. However, rhodopsin monomers were identified as the smallest functional receptor unit capable of catalyzing nucleotide exchange in G_t (32,33). Khorana and coworkers used a crosslinking approach to probe the relative orientation of G_t and R^* . They modified

[†]This invited paper is part of the Symposium-in-Print: Photoreceptors and Signal Transduction.

[‡]Yihui Chen and Rolf Herrmann contributed equally to this study

[¶]Current address: Rolf Herrmann, Duke University Eye Center, Durham, NC.

^{*}Current address: Nathan Fishkin, Immunogen, Inc., Cambridge, MA.

^{*}Corresponding authors email: kn5@columbia.edu (Koji Nakanishi), oliver.ernst@charite.de (Oliver P. Ernst)

© 2008 The Authors. Journal Compilation. The American Society of Photobiology 0031-8655/08

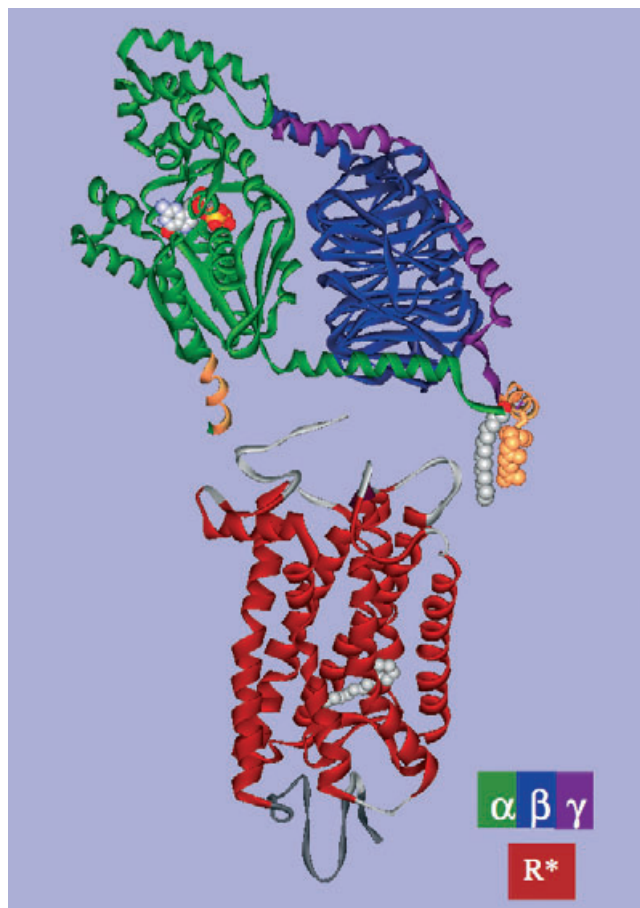


Figure 1. Interface between the heterotrimeric G protein transducin (G_t) and its receptor rhodopsin. G_t (pdb entry 1GOT) consists of the nucleotide-binding $G_t\alpha$ subunit and the $G_t\beta\gamma$ heterodimer. The GPCR rhodopsin (pdb entry 1L9H) contains the chromophore 11-*cis*-retinal (gray, space-filling model) linked *via* a Schiff base to Lys-296. The lipid modifications and the C-terminal regions of $G_t\alpha$ and $G_t\gamma$ as well as the N-terminus of $G_t\alpha$ were modeled (19). C-terminal regions shown in orange are key interaction sites for R^* .

particular cysteines on rhodopsin's cytoplasmic surface with two different heterobifunctional crosslinking reagents, a photoactivatable and a chemically preactivated one (34,35). In their study, G_t could be crosslinked from a variety of different sites on rhodopsin's second and third cytoplasmic loops with each of these reagents. This was consistent with earlier reports that these loops are involved in G protein interaction (for a review, see Hamm [11]). When Cys-240 on rhodopsin's third cytoplasmic loop was modified with a crosslinker, the cross-linked counterparts on G_t were analyzed using mass spectrometry and identified as amino- and carboxyl-terminal regions of $G_t\alpha$. However, no crosslinking products could be identified for the C-terminal region of $G_t\gamma$, leaving the question open as to where this G_t key binding site interacts with R^* . Therefore, our study aims to apply the photoaffinity labeling approach to the $G_t\gamma(60-71)$ far binding site. Here we report the design of novel, suitably modified peptides corresponding to $G_t\gamma(60-71)$ far containing isotope-coded photolabile groups to facilitate receptor fragment identification by mass spectrometry. We discuss the synthesis and present R^* binding data of these peptides.

MATERIALS AND METHODS

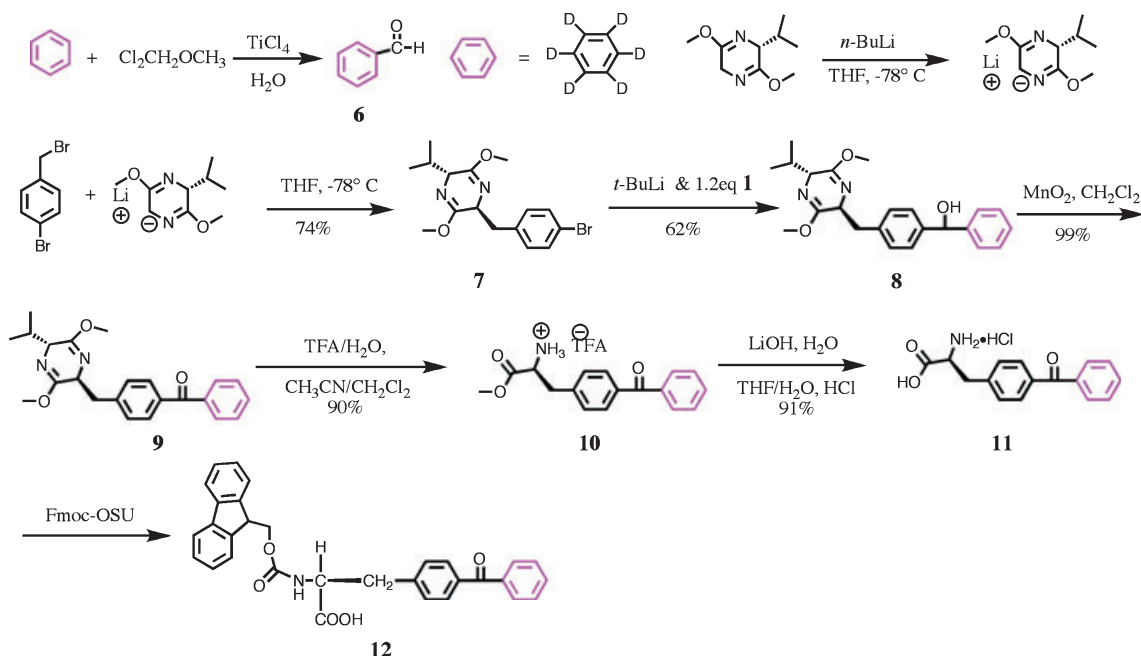
General experimental procedure. THF and diethyl ether were distilled from sodium/benzophenone ketyl. Methylene chloride was distilled over CaH_2 . All other reagents and starting materials were purchased and used as received (Aldrich, St. Louis, MO). Reactions were monitored by analytical TLC using silica gel 60 F254 plates and spots were visualized by UV (254 nm) or oxidative stain (PMA). Flash column chromatography was performed using silica gel (230–400 mesh). Analytical HPLC was performed on a Waters instrument with UV detector (200–700 nm) using a C18 reverse-phase column (4.6 mm \times 150 mm; Waters) to analyze synthetic $G_t\gamma$ -derived peptides. Water and acetonitrile were used as eluents in various gradient programs at a flow of 0.6 mL min^{-1} . $^1\text{H-NMR}$ spectra were recorded with Bruker (300 or 400 MHz) spectrometers. The chemical shifts are expressed in p.p.m. (d) downfield from tetramethylsilane (in CDCl_3). UV-Vis spectra were recorded at 25°C in a Perkin-Elmer Lambda 40 spectrophotometer. Mass spectra were measured on a JEOL KMS-HX110/100A HF mass spectrometer under FAB conditions.

Peptide synthesis. Peptide synthesis was carried out on a TentaGel resin (Rapp Polymere, Tübingen), building up the sequence from the C-terminus to the N-terminus using Fmoc-protected amino acids. After purification, peptides were lyophilized and stored at -20°C under nitrogen. Immediately before the experiments, the peptides were dissolved in appropriate buffers or deionized water and adjusted to pH 7 to obtain stock solutions of 1–10 mM. Peptide farnesylation was carried out as follows: 5 μM peptide was dissolved in 50% *n*-propyl alcohol and Na_2CO_3 was added to a final concentration of 20 mM. The solution was then treated with 30 μM farnesyl bromide in a 10% solution of *n*-propyl alcohol for 18–24 h at room temperature in the dark. Farnesylated peptides were purified by reversed phase chromatography using a PepRPC fast protein liquid chromatography column (Pharmacia Biotech, Inc.) using a linear (0–100%) gradient of acetonitrile in water containing 0.1% trifluoroacetic acid (TFA). The molecular weight of purified peptides was determined by electrospray mass spectrometry using a Vestec VT 201 mass spectrometer.

Meta II stabilization assay. The amount of “Extra MII” was monitored by time-resolved UV-Vis spectroscopy using a dual wavelength spectrophotometer (Shimadzu UV300). Recorded traces represent readings of an absorbance difference ($A_{380\text{nm}} - A_{417\text{nm}}$; absorption maximum of MII and isosbestic point between MI and MII) from the samples containing 10 μM of washed rod outer segment membranes (prepared as in Herrmann *et al.* [19]). All measurements were made in 100 mM Na-Hepes pH 7.9, 50 mM NaCl, 1 mM DTT, 1 mM MgCl_2 , 1 mM EDTA at 4°C. Cuvette path length was 2 mm. Twelve percent of rhodopsin was flash-activated by 500 ± 20 nm light. Values of half-maximal saturation (EC_{50} values) were obtained by fitting the dose-response curves to the following equation: $y = A x^n / (\text{EC}_{50}^n + x^n)$, with x as the peptide concentration, y the amount of “Extra MII,” *i.e.* the amplitude difference between the peptide or G_t induced “Extra MII” signal and the reference signal (no peptide or G_t added). A is the amount of maximal “Extra MII” formed and n the Hill coefficient. Except for the data resulting from peptide 4 (Fig. 5, $n = 1.5$), n was set to 1 in all fits.

Benzaldehyde (d5) 6. To a stirred solution of 468 mg (6 mmol) benzene (d6) in 10 mL of dichloromethane, 1.52 g (12 mmol) of titanium (IV) chloride was added at 0°C in very slow speed, then followed by drop-wise addition of 690 mg (6 mmol) freshly distilled dichloromethyl methyl ether (Scheme 1). After 25 min, the reaction mixture was warmed up to room temperature, stirred for another 1 h and poured into 10 g ice water. The mixture was extracted with dichloromethane three times, and the combined organic layers were washed with 5% aqueous NaHCO_3 and dried over sodium sulfate. The residue was purified by chromatography on silica gel (hexane:ethyl acetate 6:1) to give the pure compound 550 mg (81%). $^1\text{H NMR}$ (CDCl_3 , 300 MHz): δ 10.00 (s, 1 H); MS m/z 107.4, $[\text{M} + \text{H}^+]$ calcd. for $\text{C}_7\text{D}_5\text{H}_7\text{O}$ 106.1.

(2S,5R)-2-(4-bromobenzyl)-5-isopropyl-3,6-dimethoxy-2,5-dihydropyrazine 7. To a solution of (R)-2-isopropyl-3,6-dimethoxy-2,5-dihydropyrazine (1.5 g, 8 mmol) in THF (25 mL), was added *n*-BuLi (4.2 mL, 1.5 M in hexane) at -78°C drop-wise. After stirring for 15 min, a solution of 4-bromobenzyl bromide (2.5 g, 10.0 mmol) in THF (4 mL) was added drop-wise. The resulting mixture was stirred for 3 h at -78°C . After removal of THF, the residue was



Scheme 1. Enantioselective synthesis of Fmoc-protected 4-benzoyl-L-phenylalanine.

diluted with methylene chloride (60 mL). The organic layer was washed with 5% sulfuric acid, water and brine, then dried and concentrated *in vacuo*. Purification by chromatography on silica gel (ethyl acetate:hexane = 1:7 by volume), afforded compound 7 as a single diastereomer (100% de, 2.54 g, 90%) as a white solid: $[\alpha]_D^{25} = 40.2$ (CH_2Cl_2); $^1\text{H NMR}$ (CDCl_3 , 300 MHz) δ 7.31 (d, $J = 8.4$ Hz, 2H), 6.95 (d, $J = 8.4$ Hz, 2H), 4.28 (dd, $J = 8.7$, 3.5 Hz, 1H), 3.70 (s, 3H), 3.66 (s, 3H), 3.40 (t, $J = 3.5$ Hz, 1H), 3.03 (d, $J = 4.8$ Hz, 2H), 2.15 (m, 1H), 0.95 (d, $J = 6.8$ Hz, 3H), 0.61 (d, $J = 6.8$ Hz, 3H); MS m/z 353.1, [M 100%] calcd. for $\text{C}_{16}\text{H}_{21}\text{N}_2\text{O}_2$ 353.3.

(4-(((2*S*,5*R*)-5-isopropyl-3,6-dimethoxy-2,5-dihydropyrazin-2-yl)methyl)phenyl)(phenyl)methanol (*d5*) 8. *t*-Butyllithium (4.65 mL, 7.8 mmol, 1.7 M in pentane) was added drop-wise at -78°C to a solution of bromide 7 (1.65 g, 4.65 mmol) in distilled THF (50 mL). After 15 min, a solution of aldehyde 6 (1.0 g, 9.3 mmol) in distilled THF (8 mL) was slowly cannulated into the reaction mixture. The mixture was stirred for an additional 4 h at the same temperature. A saturated ammonium chloride solution was added and the mixture warmed to RT. The volatiles were removed *in vacuo* and the residue taken up in ethyl acetate and washed once with water. The aqueous layer was extracted three times with ethyl acetate. The combined organic extracts were dried, concentrated, and the residue purified by chromatography on silica gel (hexane:ethyl acetate 8:1) to furnish the desired diastereomeric alcohols 8 (975 mg, 55%) as a colorless oil: $^1\text{H NMR}$ (CDCl_3 , 300 MHz) δ 7.20 (d, $J = 8.1$ Hz, 1H), 7.04 (d, $J = 8.1$ Hz, 1H), 6.90 (d, $J = 8.5$ Hz, 1H), 6.62 (d, $J = 8.5$ Hz, 1H), 5.78 (d, $J = 3.1$ Hz, 1H), 4.28 (m, 1H), 3.70 (d, $J = 4.9$ Hz, 3H), 3.66 (d, $J = 3.2$ Hz, 3H), 3.27 (dd, $J = 10.8$, 3.4 Hz, 1H), 3.06 (d, $J = 4.8$ Hz, 2H), 2.40 (d, $J = 3.6$ Hz, OH), 2.14 (m, 1H), 0.94 (m, 3H), 0.61 (dd, $J = 4.5$, 2.2 Hz, 3H); MS m/z 386.1, [M + H^+] calcd. for $\text{C}_{23}\text{D}_5\text{H}_{28}\text{N}_2\text{O}_3$ 385.2.

(4-(((2*S*,5*R*)-5-isopropyl-3,6-dimethoxy-2,5-dihydropyrazin-2-yl)methyl)phenyl)(phenyl)methanone (*d5*) 9. Manganese dioxide (3.0 g, 34.5 mmol) was added in one portion at 0°C to a solution of benzylated alcohol 8 (0.45 g, 1.2 mmol) in methylene chloride (50 mL). The mixture was stirred overnight at RT, then filtered through Celite and concentrated *in vacuo* to yield 421.5 mg (99%) of ketone 9 as white crystals: $^1\text{H NMR}$ (CDCl_3 , 300 MHz) δ 7.68 (d, $J = 8.3$ Hz, 2H), 7.23 (d, $J = 8.3$ Hz, 2H), 4.36 (dd, $J = 5.1$, 2.5 Hz, 1H), 3.73 (s, 3H), 3.68 (s, 3H), 3.44 (t, 3.4 Hz, 1H), 3.20 (d, $J = 5.3$ Hz, 2H), 2.18 (m, 1H), 0.97 (d, $J = 6.8$ Hz, 3H), 0.64 (d, $J = 6.7$ Hz, 3H); MS m/z 390.5, [M + H^+] calcd. for $\text{C}_{23}\text{D}_5\text{H}_{26}\text{N}_2\text{O}_3$ 388.7.

(*S*)-methyl 2-amino-3-(4-(phenylcarbonyl)phenyl)propanoate (*d5*) 10. TFA (3.3 mmol, 0.1 N in water, 3 equiv.) was added to a solution of compound 9 (0.40 g, 1.1 mmol) in a mixture of methylene chloride (3 mL) and acetonitrile (30 mL). The resulting mixture was stirred at RT for 3 h. Acetonitrile and TFA were removed *in vacuo* to produce a suspension of the methyl ester 10 and (*D*)-valine methyl ester which remained in the aqueous phase: $^1\text{H NMR}$ (CDCl_3 , 300 MHz) δ 8.45 (br, 2H, NH_2) 7.68 (d, $J = 8.1$ Hz, 2H), 7.33 (d, $J = 8.1$ Hz, 2H), 4.30 (t, $J = 6.6$ Hz, 1H), 3.68 (s, 3H), 3.35 (d, $J = 6.6$ Hz, 2H); MS m/z 289.4, [M 100%] calcd. for $\text{C}_{17}\text{D}_5\text{H}_{18}\text{NO}_3$ 289.3.

(*S*)-2-amino-3-(4-(phenylcarbonyl)phenyl)propanoic acid (*d5*) 11. (*S*)-methyl 2-amino-3-(4-(phenylcarbonyl)phenyl)propanoate 10 (0.29 g, 1.0 mmol) was dissolved in 50 mL of THF. An aqueous solution of LiOH· H_2O (115 mg, 3.0 mmol) in 10 mL of water was added at RT and the mixture stirred for 4–5 min. Following neutralization of the mixture with 6 N HCl to pH = 3, THF was evaporated *in vacuo*. A white precipitate of the amino acid-HCl salt appeared on concentration that was cooled to 0°C for 5 h, then filtered, washed with chilled water two times and ether three times, and dried under high vacuum over P_2O_5 overnight (yield = 0.29 g, 99%): $^1\text{H NMR}$ (CD_3OD , 300 MHz) δ 7.93 (d, $J = 8.1$ Hz, 2H), 7.65 (d, $J = 8.1$ Hz, 2H), 3.58 (dd, $J = 10.0$, 4.6 Hz, 1H), 3.34 (d, $J = 8.4$ Hz, 1H), 3.30 (d, $J = 8.4$ Hz, 1H); MS m/z 275.0, [M + H^+] calcd. for $\text{C}_{16}\text{D}_5\text{H}_{15}\text{NO}_3$ 274.3.

RESULTS AND DISCUSSION

Photolabile groups at the N-terminus of the G_{17} (60-71)far peptide

The native G_{17} (60-71)far peptide is shown in Fig. 2. Photolabile analogs were prepared with a photolabile benzophenone group either at position A, the peptide's N-terminus, or at position B, Phe-64. Position A was chosen because the aspartate amino group of G_{17} (60-71)far could be directly

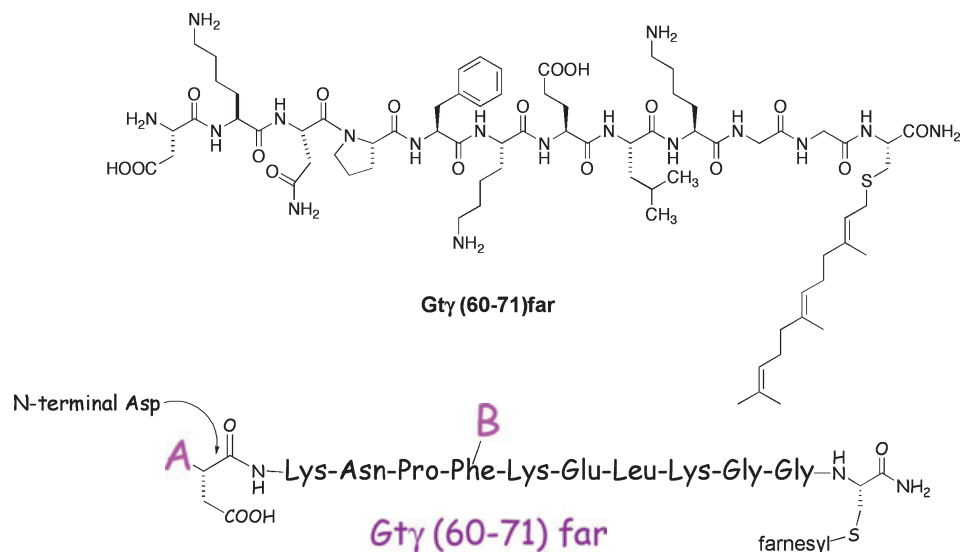


Figure 2. The G_{T_I}(60-71)far peptide (DKNPFKELKGGC-farnesyl) is modified to contain a photolabile benzophenone at positions A or B.

coupled to commercially available p-benzoyl-L-phenylalanine (Bpa) or 4-(para-bromobenzoyl)benzoic acid during peptide synthesis. After deprotection, resin removal and farnesylation, the respective photolabile peptides **1** and **2** were in hand (Fig. 3). The 4-(para-bromobenzoyl)benzoic acid group in peptide **2** was chosen to introduce a marker for mass spectrometric analysis. Crosslinking products containing this peptide would yield double peaks split by 2 *m/z* units due to the bromine isotope pattern.

To obtain peptide **3**, 4-benzoylbenzoic acid was coupled to (*S*)-malic acid-modified G_{T_I}(61-71) on the resin (malic acid replacing Asp-60), followed by deprotection, resin removal and farnesylation. An ester linkage of the photolabile group could allow aminolysis and *e.g.* amidation with 5-amino-methylfluorescein for fluorescent labeling of crosslinking products.

We tested the binding affinities of peptides **1–3** to light-activated rhodopsin by using the “Extra MII” stabilization

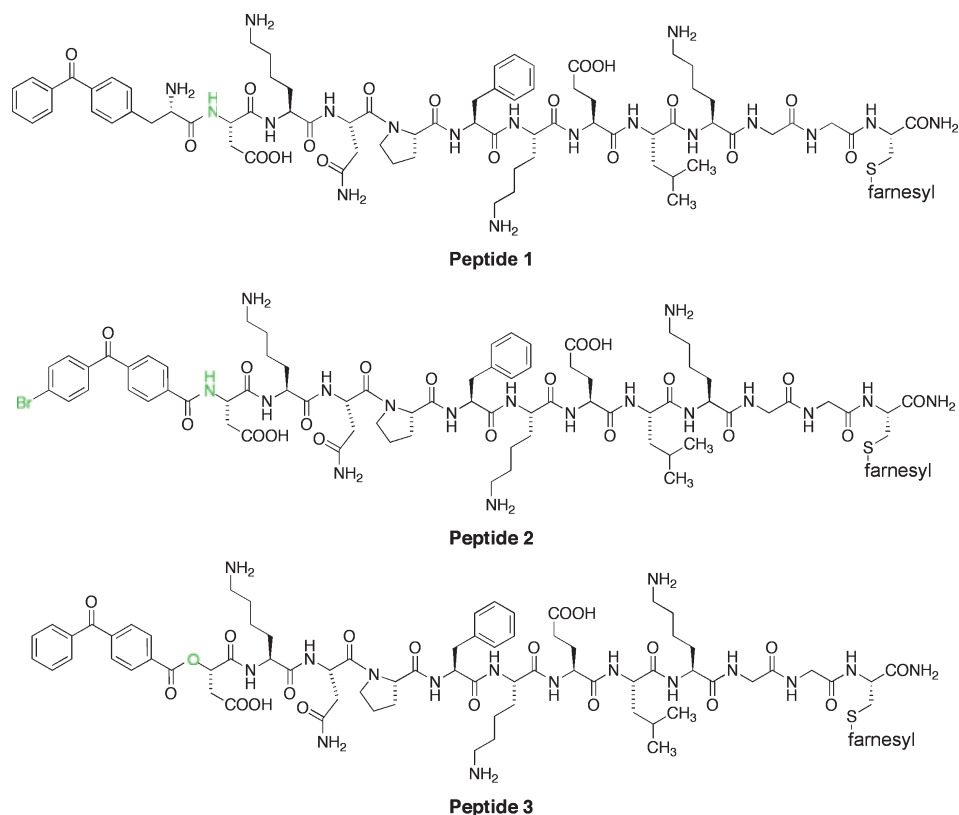


Figure 3. Derivatives of the G_{T_I}(60-71)far peptide with benzophenone modifications at the N-terminus.

assay (36,37). Flash activation of rhodopsin leads to an equilibrium between the inactive photoproduct metarhodopsin I (MI) and its successor, the active form metarhodopsin II (MII) that is capable of binding and activating G_t . Under the conditions of the “Extra MII” assay (4°C, pH 8), the MI/MII equilibrium is on the side of MI. Binding of added G_t or peptides derived from the C-termini of $G_{t\alpha}$ or farnesylated $G_{t\gamma}$, respectively, stabilize MII. They do so at the expense of MI and thereby shift the MI/MII equilibrium to the side of MII (Extra MII) (36,37). As MI and MII can be distinguished based on their different absorption maxima (MI at 480 nm and MII at 380 nm), stabilization of MII is monitored by detecting the absorption difference $\Delta A_{380} - \Delta A_{417}$ (“Extra MII”; 417 nm representing the isosbestic point between MI and MII). Using this spectral assay, we investigated the MII affinities of the synthesized peptides 1–3 (Fig. 4). Unmodified $G_{t\gamma}(60-71)$ far peptide stabilized MII in a concentration-dependent manner (Fig. 4a) with an EC_{50} value of 91 μM , in agreement with earlier determinations (17,18). Peptides 1 and 2 failed to stabilize MII at similar concentrations (Fig. 4c,d), indicating that N-terminal modification of $G_{t\gamma}(60-71)$ far may lead to a loss of interaction with MII. Although unspecific binding to the G protein cannot be excluded, it is conceivable that for these peptides the photoproduct specificity is changed, *i.e.* that they also recognize MI or earlier photoproducts even including the ground state of rhodopsin. Competition experiments in which peptide 2 competed against G_t in the “Extra MII” assay indicate such a behavior (Fig. 4c). In the presence of

sufficiently high concentrations of peptide 2 (250 and 500 μM) MII stabilization by G_t was significantly reduced. Interestingly, the rate of MII formation (see the rising phase of the traces in Fig. 4c) is decreased when peptide 2 was added (magenta and yellow traces compared to green trace in Fig. 4c). This observation further supports the conclusion that peptide 2 binds to rhodopsin photoproducts other than MII or the rhodopsin ground state. By doing so, the fraction of MI available to react into the MII species is reduced, and therefore the apparent MII formation rate is decreased.

In the case of peptide 3, “Extra MII” was formed with an EC_{50} value of about 20 μM . However, the maximal amplitude of the “Extra MII” signal under saturating peptide concentrations was only about 20% compared to the $G_{t\gamma}(60-71)$ far (Fig. 4b,d), suggesting that the preference for MII is reduced, however, in a far less pronounced manner compared to peptides 1 and 2. Interestingly, also peptide 3 lacking the benzophenone ester showed a reduced “Extra MII” amplitude (data not shown), indicating that the replacement of Asp-60 by malic acid affects the MI/MII specificity of $G_{t\gamma}(60-71)$ far as well.

Substitution of Phe-64 in $G_{t\gamma}(60-71)$ far with benzoylphenylalanine

In order to circumvent the problems with poor MII stabilization of the N-terminally modified peptides, Phe-64 in $G_{t\gamma}(60-71)$ far was considered as a position for introduction of a

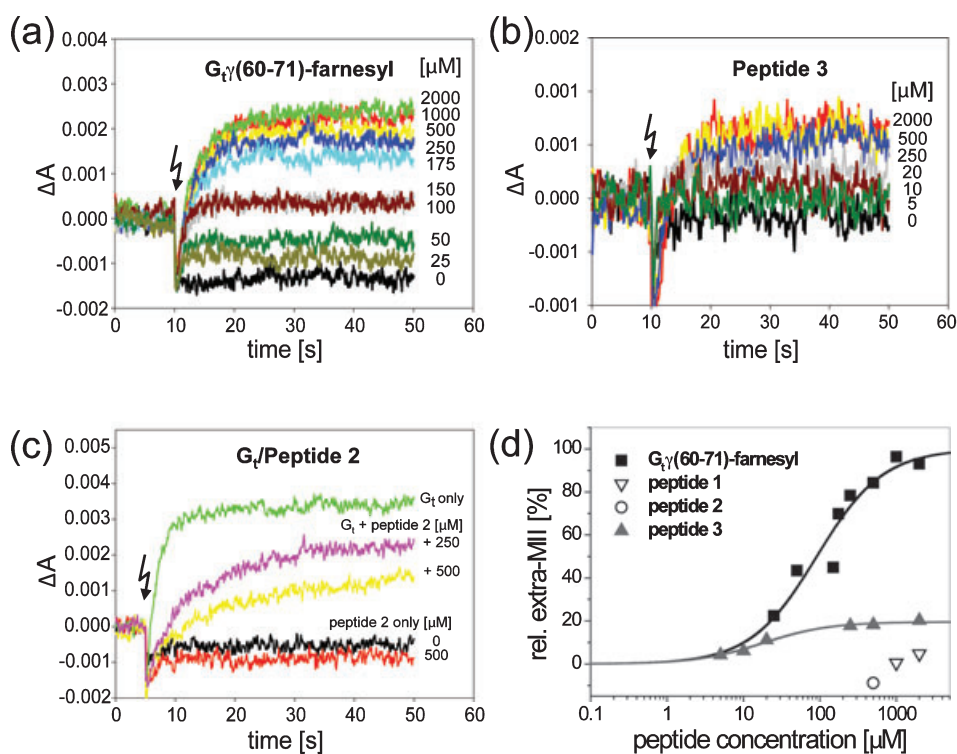


Figure 4. Probing the rhodopsin binding properties of modified $G_{t\gamma}(60-71)$ far peptides containing a benzophenone moiety at the N-terminus by the “Extra MII” assay. Stabilization of MII by increasing concentrations of the native $G_{t\gamma}(60-71)$ far peptide (a) or peptide 3 (b) is measured as an increase in relative UV-Vis absorption (absorption change at 380 nm minus the absorption change at 417 nm) after flash activation of rhodopsin (flash symbol). MII binding of G_t (upper trace, green) is inhibited in the presence of peptide 2 (magenta and yellow) which fails to stabilize MII by itself (c, bottom trace, red). Dose-response curves of the “Extra MII” data for all peptides tested (d). Plotted are “Extra MII” amplitude versus peptide concentration. No MII binding is observed for peptides 1 and 2. Data are normalized to the maximal amplitude obtained for the $G_{t\gamma}(60-71)$ far peptide.

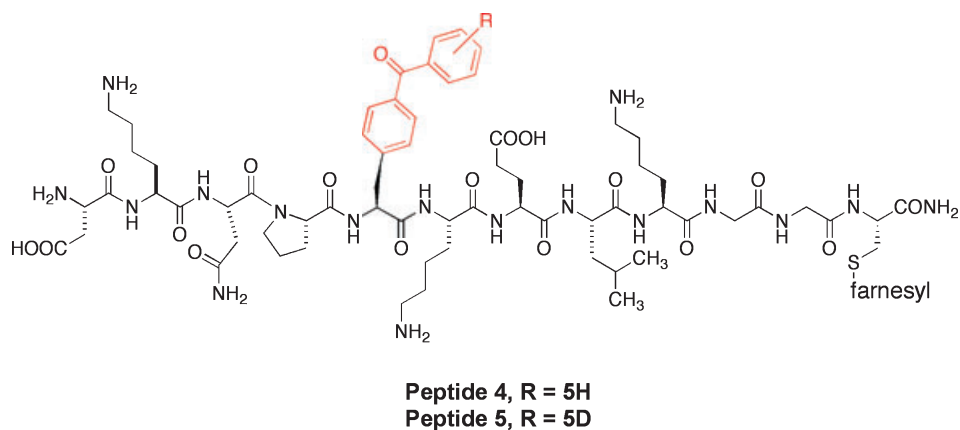


Figure 5. $G_{T\gamma}(60-71)$ far peptides modified at position Phe-64, which is replaced by 4-benzoyl-L-phenylalanine (Bpa).

para-benzoyl group by substitution with Bpa (4-benzoyl-L-phenylalanine). Such a replacement is appealing as it would represent a relatively small modification of the native peptide. In order to facilitate mass spectrometric analysis of future photocrosslinking products, attention was turned to the synthesis of peptides **4** and **5**, a pentadeuterated version of peptide **4** (Fig. 5). Mixing both peptides in a 1:1 ratio for photocrosslinking experiments with R^* should facilitate identification of crosslinked products by the occurrence of double peaks split by 5 m/z units due to the isotope coding. Peptide **4** was synthesized using commercially available Fmoc-4-benzoyl-L-phenylalanine. For synthesis of peptide **5**, a corresponding pentadeuterated Fmoc-4-benzoyl-L-phenylalanine building block was made (Scheme 1; for synthesis details, see Materials and Methods).

To synthesize pentadeuterated 4-benzoyl-L-phenylalanine, we used a bulky chiral ester to control diastereoselectivity (38). The entire synthesis of 4-benzoyl-L-phenylalanine was carried out in a straightforward manner using the commercially available chiral auxiliary known as Schollkopf's reagent (Scheme 1). Thus, for the synthesis of peptide **5**, *p*-bromobenzyl bromide was coupled to (*R*)-Schollkopf's reagent, (2*R*)-2-isopropyl-3,6-dimethoxy-2,5-dihydropyrazine, to give (*S,R*) bislactim ether **7**, which was obtained as a single diastereomer (100% de) as indicated by the NMR and TLC analyses of the

crude isolate after work-up. Halogen-metal exchange of **7** at -78°C followed by the addition of pentadeuterated benzaldehyde **6** (PDB, obtained in 81% yield) gave a mixture of diastereomeric benzhydryl alcohols (compound **8**), which, after purification, could be readily oxidized to benzophenone **9**. Mild acid hydrolysis of **9** to aminoester **10** was followed by a very rapid reaction with a 1 M excess of LiOH in $\text{H}_2\text{O}/\text{THF}$ to give amino acid **11**; the Fmoc-protected amino acid **12** was obtained by reaction of Fmoc-OSU with compound **11** and used for synthesis of peptide **5**.

Phe-64 was shown to be important for interaction of $G_{T\gamma}(60-71)$ far with R^* (17,39–41). Therefore, we tested the binding affinities of peptide **4** to light-activated rhodopsin by using the “Extra MII” assay as described above. Peptide **4** stabilized MII in a concentration-dependent manner with an EC_{50} value of 60 μM (Fig. 6). This value was approximately 30% lower compared to the parent $G_{T\gamma}(60-71)$ far peptide ($\text{EC}_{50} = 91 \mu\text{M}$), indicating a slight affinity increase in peptide **4** for MII. Importantly, the para-benzoyl modification of the $G_{T\gamma}(60-71)$ far peptide at position 64 showed little effect on the amplitude of the “Extra MII” signals, indicating that the specificity of the peptide for MII was not affected. In contrast to the results from the competition experiment performed with G_T and peptide **2** (Fig. 4c), the observed initial rates of MII formation in this set of measurements were identical over the

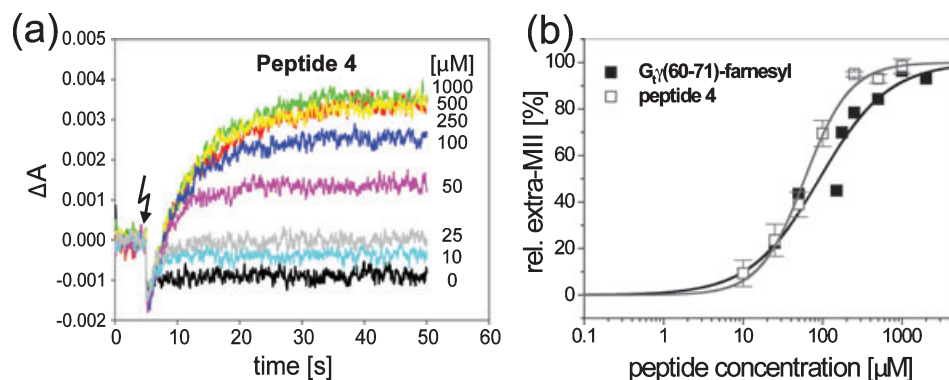


Figure 6. MII stabilization by peptide **4**, the F64Bpa substituted $G_{T\gamma}(60-71)$ far analog, measured by the “Extra MII” assay. “Extra MII” formation by increasing concentrations of peptide **4** (a). Dose–response curves of the “Extra MII” amplitudes of peptide **4** and for comparison $G_{T\gamma}(60-71)$ far peptide (b). Shown are averages of three different measurements. Error bars indicate SEM.

whole measured peptide concentration range. This indicates that conformational changes in rhodopsin were rate-limiting and that MII was formed from its precursor MI.

There are other examples in the literature where modification with Bpa slightly increased ligand affinity for the respective receptor. An N-formyl peptide ligand modified with a Bpa moiety was reported to have a two-fold increased affinity for its human neutrophil formyl peptide receptor (42). Also, the attachment of a benzophenone probe to Ginkgolide B at the 10-OH group, *via* either a methylene or carboxy linkage, increased the ligand's ability to inhibit the platelet-activating factor receptor by more than three times (43).

CONCLUSION

We found that substituting Phe-64 of the G_{iγ}(60-71)far peptide by 4-benzoyl-L-phenylalanine (Bpa) yields a photolabile peptide which retains its affinity for the active MII state. This peptide should be suited to determine the binding site of G_{iγ}(60-71)far on the activated receptor by photocrosslinking and subsequent receptor fragmentation followed by mass spectrometric analysis. The great advantage of this novel MII-recognizing peptide is the pentadeuterated benzophenone moiety, which can be readily used in a mixture with the nondeuterated twin peptide. This will lead to a facilitated MS analysis of crosslinked samples, as labeled fragments of the digested receptor will appear as double peaks in the MS spectra. These characteristics make such peptides excellent candidates for protein labeling studies in G protein research and more general applications such as protein-protein interaction studies.

Acknowledgements—We thank Klaus Peter Hofmann for helpful discussions and critical reading of the manuscript. We acknowledge support from NIH grants GM 36564 (to K.N.) and DFG Sfb449 (to O.P.E.).

REFERENCES

- Hamm, H. E. (1998) The many faces of G protein signaling. *J. Biol. Chem.* **273**, 669–672.
- Wess, J. (1997) G-protein-coupled receptors: Molecular mechanisms involved in receptor activation and selectivity of G-protein recognition. *FASEB J.* **11**, 346–354.
- Schwalbe, H. and G. Wess (2002) Dissecting G-protein-coupled receptors: Structure, function, and ligand interaction. *ChemBiochem* **3**, 915–919.
- Lambright, D. G., J. Sondek, A. Bohm, N. P. Skiba, H. E. Hamm and P. B. Sigler (1996) The 2.0 Å crystal structure of a heterotrimeric G protein. *Nature* **379**, 311–319.
- Palczewski, K., T. Kumasaka, T. Hori, C. A. Behnke, H. Motoshima, B. A. Fox, I. Le Trong, D. C. Teller, T. Okada, R. E. Stenkamp, M. Yamamoto and M. Miyano (2000) Crystal structure of rhodopsin: A G protein-coupled receptor. *Science* **289**, 739–745.
- Okada, T., Y. Fujiyoshi, M. Silow, J. Navarro, E. M. Landau and Y. Shichida (2002) Functional role of internal water molecules in rhodopsin revealed by x-ray crystallography. *Proc. Natl Acad. Sci. USA* **99**, 5982–5987.
- Li, J., P. C. Edwards, M. Burghammer, C. Villa and G. F. Schertler (2004) Structure of bovine rhodopsin in a trigonal crystal form. *J. Mol. Biol.* **343**, 1409–1438.
- Bohm, A., R. Gaudet and P. B. Sigler (1997) Structural aspects of heterotrimeric G-protein signaling. *Curr. Opin. Biotechnol.* **8**, 480–487.
- Bourne, H. R. (1997) How receptors talk to trimeric G proteins. *Curr. Opin. Cell Biol.* **9**, 134–142.
- Iiri, T., Z. Farfel and H. R. Bourne (1998) G-protein diseases furnish a model for the turn-on switch. *Nature* **394**, 35–38.
- Hamm, H. E. (2001) How activated receptors couple to G proteins. *Proc. Natl Acad. Sci. USA* **98**, 4819–4821.
- Oldham, W. M., N. Van Eps, A. M. Preininger, W. L. Hubbell and H. E. Hamm (2006) Mechanism of the receptor-catalyzed activation of heterotrimeric G proteins. *Nat. Struct. Mol. Biol.* **13**, 772–777.
- Yeagle, P. L. and A. D. Albert (2003) A conformational trigger for activation of a G protein by a G protein-coupled receptor. *Biochemistry* **42**, 1365–1368.
- Cherfils, J. and M. Chabre (2003) Activation of G-protein Galpha subunits by receptors through Galpha-Gbeta and Galpha-Ggamma interactions. *Trends Biochem. Sci.* **28**, 13–17.
- Chabre, M. and M. le Maire (2005) Monomeric G-protein-coupled receptor as a functional unit. *Biochemistry* **44**, 9395–9403.
- Shichida, Y. and T. Morizumi (2007) Mechanism of G-protein activation by rhodopsin. *Photochem. Photobiol.* **83**, 70–75.
- Kisselev, O., A. Pronin, M. Ermolaeva and N. Gautam (1995) Receptor-G protein coupling is established by a potential conformational switch in the beta gamma complex. *Proc. Natl Acad. Sci. USA* **92**, 9102–9106.
- Kisselev, O. G., C. K. Meyer, M. Heck, O. P. Ernst and K. P. Hofmann (1999) Signal transfer from rhodopsin to the G-protein: Evidence for a two-site sequential fit mechanism. *Proc. Natl Acad. Sci. USA* **96**, 4898–4903.
- Herrmann, R., M. Heck, P. Henklein, P. Henklein, C. Kleuss, K. P. Hofmann and O. P. Ernst (2004) Sequence of interactions in receptor-G protein coupling. *J. Biol. Chem.* **279**, 24283–24290.
- Herrmann, R., M. Heck, P. Henklein, K. P. Hofmann and O. P. Ernst (2006) Signal transfer from GPCRs to G proteins: Role of the Galpha N-terminal region in rhodopsin-transducin coupling. *J. Biol. Chem.* **281**, 30234–30241.
- Nanoff, C., R. Koppensteiner, Q. Yang, E. Fuerst, H. Ahorn and M. Freissmuth (2006) The carboxyl terminus of the Galpha subunit is the latch for triggered activation of heterotrimeric G proteins. *Mol. Pharmacol.* **69**, 397–405.
- Nikiforovich, G. V. and G. R. Marshall (2006) 3D modeling of the activated states of constitutively active mutants of rhodopsin. *Biochem. Biophys. Res. Commun.* **345**, 430–437.
- Hamm, H. E., D. Deretic, A. Arendt, P. A. Hargrave, B. Koenig and K. P. Hofmann (1988) Site of G protein binding to rhodopsin mapped with synthetic peptides from the alpha subunit. *Science* **241**, 832–835.
- Kisselev, O. G., J. Kao, J. W. Ponder, Y. C. Fann, N. Gautam and G. R. Marshall (1998) Light-activated rhodopsin induces structural binding motif in G protein alpha subunit. *Proc. Natl Acad. Sci. USA* **95**, 4270–4275.
- Kisselev, O. G. and M. A. Downs (2003) Rhodopsin controls a conformational switch on the transducin gamma subunit. *Structure* **11**, 367–373.
- Natochin, M., M. Moussaif and N. O. Artemyev (2001) Probing the mechanism of rhodopsin-catalyzed transducin activation. *J. Neurochem.* **77**, 202–210.
- Marin, E. P., A. G. Krishna and T. P. Sakmar (2002) Disruption of the alpha 5 helix of transducin impairs rhodopsin-catalyzed nucleotide exchange. *Biochemistry* **41**, 6988–6994.
- Filipek, S., K. A. Krzysko, D. Fotiadis, Y. Liang, D. A. Saperstein, A. Engel and K. Palczewski (2004) A concept for G protein activation by G protein-coupled receptor dimers: The transducin/rhodopsin interface. *Photochem. Photobiol. Sci.* **3**, 628–638.
- Nikiforovich, G. V., C. M. Taylor and G. R. Marshall (2007) Modeling of the complex between transducin and photoactivated rhodopsin, a prototypical G-protein-coupled receptor. *Biochemistry* **46**, 4734–4744.
- Fanelli, F. and D. Dell'Orco (2005) Rhodopsin activation follows precoupling with transducin: Inferences from computational analysis. *Biochemistry* **44**, 14695–14700.
- Ciarkowski, J., M. Witt and R. Slusarz (2005) A hypothesis for GPCR activation. *J. Mol. Model.* **11**, 407–415.

32. Bayburt, T. H., A. J. Leitz, G. Xie, D. D. Oprian and S. G. Sligar (2007) Transducin activation by nanoscale lipid bilayers containing one and two rhodopsins. *J. Biol. Chem.* **282**, 14875–14881.
33. Ernst, O. P., V. Gramse, M. Kolbe, K. P. Hofmann and M. Heck (2007) Monomeric G protein-coupled receptor rhodopsin in solution activates its G protein transducin at the diffusion limit. *Proc. Natl Acad. Sci. USA* **104**, 10859–10864.
34. Cai, K., Y. Itoh and H. G. Khorana (2001) Mapping of contact sites in complex formation between transducin and light-activated rhodopsin by covalent crosslinking: Use of a photoactivatable reagent. *Proc. Natl Acad. Sci. USA* **98**, 4877–4882.
35. Itoh, Y., K. Cai and H. G. Khorana (2001) Mapping of contact sites in complex formation between light-activated rhodopsin and transducin by covalent crosslinking: Use of a chemically preactivated reagent. *Proc. Natl Acad. Sci. USA* **98**, 4883–4887.
36. Emeis, D., H. Kuehn, J. Reichert and K. P. Hofmann (1982) Complex formation between metarhodopsin II and GTP-binding protein in bovine photoreceptor membranes leads to a shift of the photoproduct equilibrium. *FEBS Lett.* **143**, 29–34.
37. Ernst, O. P., C. Bieri, H. Vogel and K. P. Hofmann (2000) Intrinsic biophysical monitors of transducin activation: Fluorescence, UV-visible spectroscopy, light scattering, and evanescent field techniques. *Methods Enzymol.* **315**, 471–489.
38. Schoellkopf, U. and H. J. Neubauer (1982) Asymmetric syntheses via heterocyclic intermediates. XII. Enantioselective synthesis of (R)-alpha amino acids using tert-leucine as chiral auxiliary reagent. *Synthesis* **1982**, 861–864.
39. Kisselev, O. G., M. V. Ermolaeva and N. Gautam (1994) A farnesylated domain in the G protein gamma subunit is a specific determinant of receptor coupling. *J. Biol. Chem.* **269**, 21399–21402.
40. Kisselev, O. G. and M. A. Downs (2006) Rhodopsin-interacting surface of the transducin gamma subunit. *Biochemistry* **45**, 9386–9392.
41. Ernst, O. P., C. K. Meyer, E. P. Marin, P. Henklein, W.-Y. Fu, T. P. Sakmar and K. P. Hofmann (2000) Mutation of the fourth cytoplasmic loop of rhodopsin affects binding of transducin and peptides derived from the carboxyl-terminal sequences of transducin a and g subunits. *J. Biol. Chem.* **275**, 1937–1943.
42. Mills, J. S., H. M. Miettinen, D. Barnidge, M. J. Vlases, S. Wimer-Mackin, E. A. Dratz, J. Sunner and A. J. Jesaitis (1998) Identification of a ligand binding site in the human neutrophil formyl peptide receptor using a site-specific fluorescent photoaffinity label and mass spectrometry. *J. Biol. Chem.* **273**, 10428–10435.
43. Stromgaard, K., D. R. Saito, H. Shindou, S. Ishii, T. Shimizu and K. Nakanishi (2002) Ginkgolide derivatives for photolabeling studies: Preparation and pharmacological evaluation. *J. Med. Chem.* **45**, 4038–4046.